A new direct power control method of the DFIG-DRWT system using neural PI controllers and four-level neural modified SVM technique

Habib Benbouhenni*[a] • Nicu Bizon[b,c,d]

[a]Faculty of Engineering and Architecture, Department of Electrical & Electronics Engineering,
Nisantasi University, 34481742 Istanbul, Turkey
[b]Faculty of Electronics, Communication and Computers, University of Pitesti, 110040 Pitesti, Romania
[c]ICSI Energy, National Research and Development Institute for Cryogenic and Isotopic Technologies,
Ramnicu Valcea, Romania
[d]Doctoral School, Polytechnic University of Bucharest, 313 Splaiul Independentei,060042 Bucharest, Romania

Abstract: Recently, direct power control (DPC) based proportional-integral (PI) controllers have become dominant for doubly fed induction generators (DFIGs) due to its simplicity and good dynamic response. But this strategy gives a high total harmonic distortion (THD) of the voltage and a large power ripple. In this paper, a new DPC method (called as NDPC-4L-NSVPWM) is proposed based on a four-level neural space vector pulse width modulation (4L-NSVPWM) and neural PI controllers for direct active and reactive powers command (DRAPC) of a DFIG integrated in a dual-rotor wind turbine (DRWT). This control scheme is based on direct reactive and active powers estimation. Theoretical principles of this strategy are presented along with simulation results. The advantages and robustness of NDPC-4L-NSVPWM control over other DPC with PI controllers (DPC-PI) are presented. The main advantages of NDPC-4L-NSVPWM strategy are relative to its good dynamic response, simplicity of the algorithm and operation at a constant switching frequency. Analysis of NDPC-4L-NSVPWM strategy based DFIG-DRWT has been done in MATLAB/Simulink software. Simulation results validate the performance of the NDPC-4L-NSVPWM strategy by evaluating the THD of current and the reduction of the ripples for the active/reactive power of DFIG-DRWTs.

*Corresponding author.
E-mail address: habib.benbouenni@nisantasi.edu.tr (Habib Benbouhenni).
Peer Review under the responsibility of Universidad Nacional Autónoma de México.

1. Introduction

Doubly fed induction generators (DFIGs) are most popular for wind energy, as they have high effectiveness Djerriri (2020), Djilali et al. (2020). Jazaeri et al. (2012), Mondal et al. (2020). The DFIG based wind turbines (DFIG-WTs), a typically employed wind power generation system, have been widely used to achieve the maximum energy conversion, smaller capacity of energy electronic devices and full controllability of reactive, and active powers of the DFIG-WT Phan et al. (2015), due to their performances such as varying speed operation. The rotor of the DFIG is fed via a rotor side inverter (RSI), while the stator circuit is connected to the grid directly Rodarte Gutierrez et al. (2021). On the other hand, many strategies have been designed for controlling the rotor converter of the DFIG-WT. In Amrane et al. (2016), the vector method (VM) strategy is the most popular method used in the command of the rotor converter for DFIG-WT. This technique is based on the SVO method (Stator Voltage Orientation) Muller et al. (2002) or an SFO method (Stator Flux Orientation) Xu and Cheng (1995). In the VC strategy, proportional-integral (PI) are used to regulate the reactive/active power of the DFIG-WT. Besides, the VM technique need accurate values of DFIG-WT parameters and rotor speed. This method gives a large THD value for the rotor/stator voltage Benbouhenni and Bizon (2021a).

To minimize the THD of the DFIG, direct flux and torque command (DFTC) have been presented in Chen et al. (2010), El Ouanjli et al. (2019), Farajpour et al. (2020). In the classical DFTC method, torque and rotor flux can be regulated by using two hysteresis controllers and lookup tables. However, direct torque technique is a robust algorithm and simple structure relative to VM strategy. This technique minimizes the THD value compared to vector command and has a good dynamic response. Similar to the DFTC strategy, a direct reactive/active power command (DRAPC) of DFIG-WT was recently proposed Izanlo et al. (2017), Jou et al. (2009), Mirzakhani et al. (2018). The basic principle of the DRAPC command was proposed by Noguchi in 1998. In the DRAPC strategy, the active and reactive powers replace the torque and rotor flux amplitude used as a controlled output in the DFTC method. In addition, the reactive and active powers can be regulated by using a lookup table and two hysteresis controllers. Also, the DRAPC technique is an easy, robust and simple method relative to the VM strategy. The DRAPC technique gives a good dynamic response and reduces the reactive and active powers ripples of the DFIG-WT. In Shehata et al. (2013), an improved DRAPC method of wind turbine driven DFIGs was presented. In Zhi and Xu (2007), the DRAPC method was proposed based on the stator flux orientation technique to reduces torque and active power undulations. In Benbouhenni (2019), a novel DRAPC strategy was designed based on the neural network algorithm and five-level inverter, where the lookup table is replaced by a neural

algorithm. In Mossa et al. (2020), active/reactive powers PI controllers and classical space vector pulse width modulation (SVPWM) strategy were combined to replace the hysteresis comparators. In Bouyekni et al. (2018), the DRAPC strategy based on a high sliding mode controller (HSMC) has been designed. In Xu et al. (2006), a DRAPC technique was proposed to command the DFIG without using a rotor position sensor. In Benbouhenni et al. (2018), a DRAPC technique was proposed using twelve sectors and neural algorithms. In Benbouhenni (2020a), two neural hysteresis comparators were proposed to minimize the active power and torque undulations of DFIG-WT controlled by the DRAPC method. In Benbouhenni et al. (2021), a novel DPC technique was proposed based on the neural HSMCmethod, where a PI of DRAPC with SVPWM technique was replaced by the NHSMC algorithm. However, this technique is simple and gives minimum power ripples compared to the conventional DRAPC method. In Benbouhenni et al. (2020), the author designs a novel DPC technique based on the neuro-fuzzy HSMC (NF-HSMC) algorithm to command DFIG-WT.

In this work, the neural DPC technique with the application of the four-level NSVPWM technique has been proposed. The original contribution of this work is the application of the four-level NSVPWM strategy in the neural DPC control scheme with DFIG-based dual-rotor wind turbine (DRWT) and performance investigation of this new control method (called below as NDPC-4L-NSVPWM).

The novelty and main contributions of this work are as follows:

1) proposal of a new direct power control method of the DFIG-DRWT using neural PI controllers and four-level neural space vector PWM technique (NDPC-4L-NSVPWM).

2) application of the NDPC-4L-NSVPWM control method with DFIG-based dual-rotor wind power (DRWP).

3) comparative performance analysis of the proposed method based on new performance indicators for the reference tracking test (RTT) and the robustness test (RT).

4) comparative investigation of the performance of the NDPC-4L-NSVPWM control method with other control method proposed in the literature.

This paper is divided into 4 Sections. In Section 1, the introduction is presented. The mathematical model of the DFIG, the DPC technique with PI controllers, the description of the four-level NSVPWM technique and the NDPC-4L-NSVPWM control method are presented in Section 2. Simulation studies are presented and discussed in Section 3 and 4. The paper is concluded with a summary.

2. Material and methods

In order to simply highlight the proposed idea, a scheme representing the design and implementation stages is

presented in Figure 1. It is worth mentioning that the designed DPC method is very simple and uncomplicated, being easily implemented based on the use of neural networks both at the level of the SVPWM controller and the PI controller to obtain a more robust DPC method. Neural networks were used in this paper due to the higher speed and accuracy of response compared to other methods, such as fuzzy logic.

2.1. Mathematical model of the DFIG

In order to generate energy from wind, we need a generator and a turbine. The latter converts wind power into mechanical power in order to rotate the generator and thus produce electric current. In this work, a DRWT was used, and this is because of its efficiency compared to a single-rotor, and also because of the value of the torque generated by it.

This turbine has been studied in several scientific works Luo and Niu (2017), Wang et al. (2019), Yahdou et al. (2020), Zhao et al. (2015). On the other hand, the mathematical model of three-phase DFIG has been formulated based on commonly used simplifying assumptions presented in detail in Zhao et al. (2015), Ayrir et al. (2020).

The fluxes equations are given as follows:

$$\begin{cases} \Psi_{dr} = MI_{ds} + L_r I_{dr} \\ \Psi_{qr} = L_r I_{qr} + MI_{qs} \\ \Psi_{qs} = MI_{qr} + L_s I_{qs} \\ \Psi_{ds} = MI_{dr} + L_s I_{ds} \end{cases} \tag{1}$$

Equation (2) represents the direct and quadrature rotor/stator voltages of the DFIG.

$$\begin{cases} V_{dr} = R_r \times I_{dr} + \frac{d}{dt} \times \Psi_{dr} - w_r \times \Psi_{qr} \\ V_{qr} = R_r \times I_{qr} + \frac{d}{dt} \times \Psi_{qr} + w_r \times \Psi_{dr} \\ V_{qs} = R_s \times I_{qs} + \frac{d}{dt} \times \Psi_{qs} + w_s \times \Psi_{ds} \\ V_{ds} = R_s \times I_{ds} + \frac{d}{dt} \times \Psi_{sd} - w_s \times \Psi_{qs} \end{cases} \tag{2}$$

Equation (3) represents the mechanical equation of the DFIG.

$$T_e = J \times \frac{d\Omega}{dt} + f \times \Omega + T_r \tag{3}$$

And:

$$T_r = 1.5\, p \times \frac{M}{L_s} (-\Psi_{sd} \times I_{rq} + \Psi_{sq} \times I_{rd}) \tag{4}$$

Equation (5) represents the reactive/active power of the DFIG.

$$\begin{cases} P_s = 1.5 \times (V_{qs} \times I_{qs} + I_{ds} \times V_{ds}) \\ Q_s = 1.5 \times (-I_{qs} \times V_{ds} + V_{qs} \times I_{ds}) \end{cases} \tag{5}$$

There are several methods used to control generators such as FOC, DTC and DPC. Each method has advantages, performances and disadvantages. In Table 1, The characteristics of the most frequently used methods are summarized. Through this table, it was noticed that the DPC strategy is among the methods that have good properties, and this is noticed through the frequent use of control, especially in the field of wind energy.

Table 1. A comparative study between the different methods used in the control of DFIG.

	DTC control	FOC strategy	Direct vector or control	DRAPC strategy	Indirect vector control	Backstepping control
Simplicity	Simple	Rather complicated	Simple	Simple	Rather complicated	Complicated
Quality of current	Acceptable	Weak	Weak	Acceptable	Weak	Good
THD	Medium	High	High	Medium	High	Medium
Dynamic response	Fast	Slow	Slow	Fast	Slow	Fast
Experimentation	Easy	Difficult	Easy	Easy	Difficult	Difficult
Controller	Hysteresis controller	PI controller	PI controller	Hysteresis controller	PI controller	-
Control of inverter	Switching table	PWM	PWM	Switching table	PWM	PWM
Robustness	Robust	Not robust	Not robust	Robust	Not robust	Robust

2.2. DPC strategy with PI controllers

The DPC-PI goal is to command the active and reactive powers of the DFIG-DRWT. In this control, reactive power is regulated using the direct axis voltage Vdr*, while the active power is regulated using the quadrature axis voltage Vqr*. This strategy is detailed in Yousefi-Talouki et al. (2019). The main advantages of the DPC-PI with the 2-level SVPWM strategy are its good dynamic response, constant switching frequency operation, and simple algorithm Mekkaoui et al. (2017). But this technique determines a high value for THD of the voltage and more powers ondulations of the DFIG-DRWT. In addition, this method is less durable, and this is due to the use of PI regulators.

As it is known, this method depends mainly on the classical DPC method or in another way is a development of the DPC technique. In this method, hysteresis comparators and switching table of classical DPC strategy are changed by PI controllers and SVM technique, respectively.

The proposed DPC-PI with SVPWM, which is proposed to reducer active and active power undulations of the DFIG-based DRWT system, is shown in Figure 2. In this technique, reactive and active powers are controlled by using two PI controllers. On the other hand, the generator inverter is controlled by the two-level SVPWM technique.
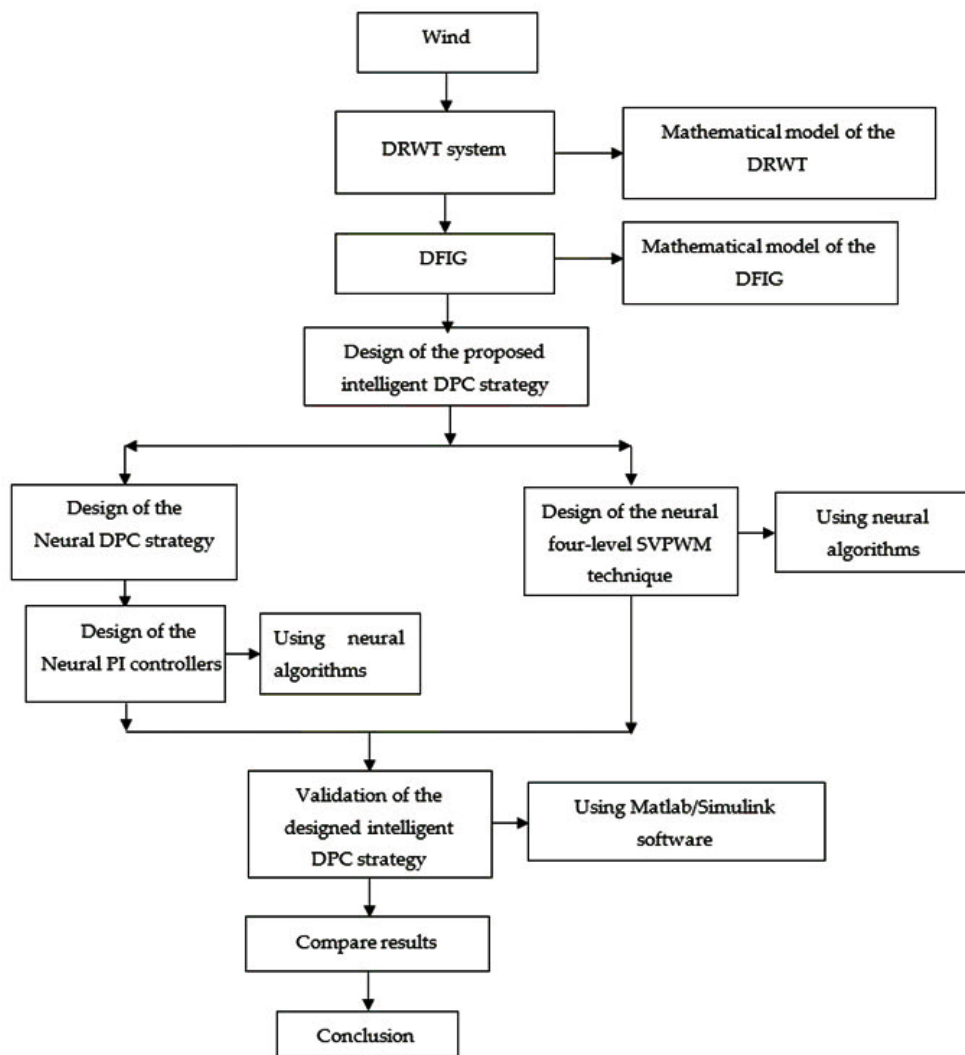

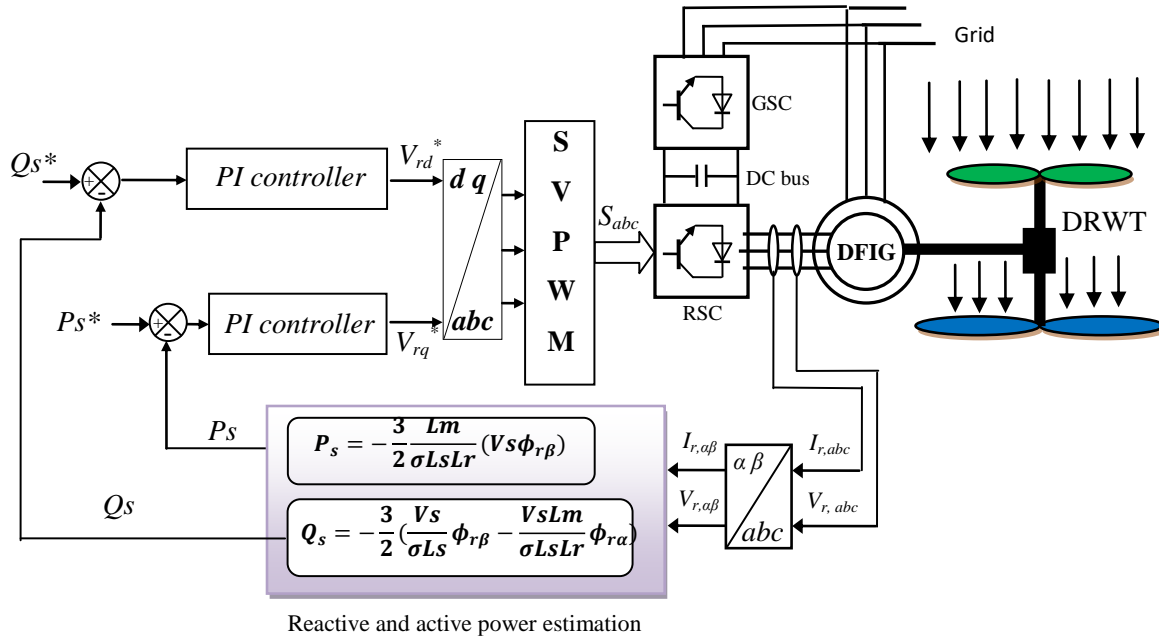Figure 1. Diagram for proposed approach.

Figure 2. DPC-PI strategy of DFIG-DRWT system.

The components of flux can be estimated by Kulothungan et al. (2019):

$$\begin{cases} \Psi_{r\alpha} = \int_0^t (V_r - R_r \times i_{r\alpha})dt \\ \Psi_{r\beta} = \int_0^t (V_r - R_r \times i_{r\beta})dt \end{cases} \quad (6)$$

The rotor flux is given by:

$$|\Psi_r| = \sqrt{\left(\Psi_{r\beta}^2 + \Psi_{r\alpha}^2\right)} \quad (7)$$

where:

$$|\overline{V}_r| = |\overline{\Psi}_r| \times w_r \quad (8)$$

Equation (9) represents the rotor angle of rotor flux:

$$\theta r = artg \frac{\Psi_{r\beta}}{\Psi_{r\alpha}} \quad (9)$$

Reactive and active powers are calculated using (10) and (11):

$$Q_s = -\frac{3}{2}\left(\frac{V_s}{\sigma \times L_s} \times \Psi_{\beta r} - \frac{V_s \times L_m}{\sigma \times L_r \times L_s}\right) \quad (10)$$

$$P_s = -\frac{3}{2}V_s \times \Psi_{r\beta} \times \frac{L_m}{\sigma \times L_r \times L_s} \quad (11)$$

$$\Psi_{s\beta} = \sigma I_{r\beta}L_r \quad (12)$$

$$\Psi_{s\beta} = \sigma I_{r\beta}L_r \quad (13)$$

$$\Psi_s = \sqrt{\Psi_{s\alpha}^2 + \Psi_{s\beta}^2} \quad (14)$$

$$\sigma = -\frac{M^2}{L_s L_r} \quad (15)$$

The use of the classical SVPWM technique offers several advantages, among which we can mention the minimization of the THD value of the current and the fact that the output voltage is 80% higher compared to the PWM technique. But this method is relatively difficult to implement because it is based on complicated control schemes that uses the calculation of the sector and the angle Kulothungan et al. (2019). In Benbouhenni (2020b), the author proposes a new SVPWM strategy of 2-level converter based on Min and Max of the 3-phase voltages. This designed strategy is easy to implement, as it is based on a simple algorithm and an uncomplicated technique compared to the SVPWM scheme. This technique is detailed in Benbouhenni and Bizon (2021b, 2021c). The two-level SVPWM technique proposed to command the two-level converter is illustrated in Figure 3.
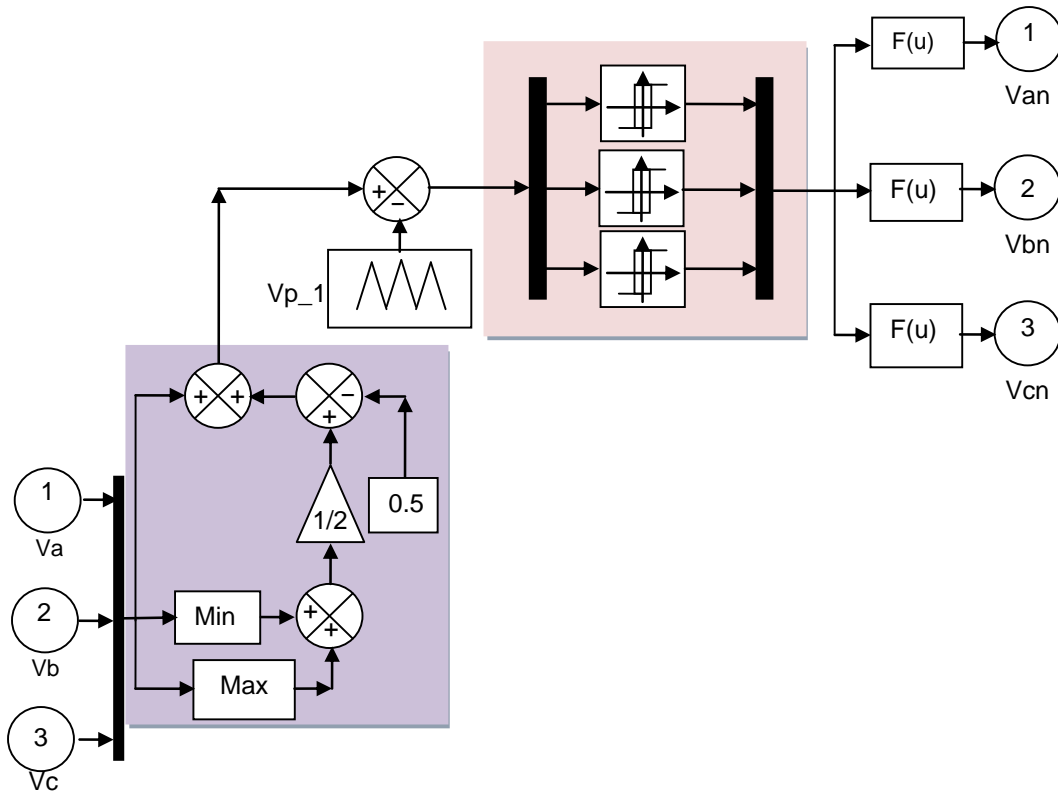
Figure 3. Two-level SVPWM strategy.

Table 2 presents a comparative study between the traditional SVM and SVM proposed in Benbouhenni (2020b). It can be said from this table, that the designed SVM technique in Benbouhenni (2020b) is a better method than the classical SVM method in terms of cost of implementation, speed of response, energy consumption and THD value. Therefore, this principle is used here for controlling a four-level inverter. Next subsectionof this paper explains the proposed neural SVPWM (NSVPWM) method for controlling a four-level inverter for an asynchronous generator (DFIG).

2.3. Four-level neural SVPWM technique

In this paper, it is suggested to use a four-level inverter for the generator rotor feeding instead of using a classic inverter in order to obtain better results. The SVPWM technique was chosen for the control of the four-level NPC inverter due to its simplicity and ease of implementation. The block diagram of the designed SVPWM technique for four-level NPC inverter is shown in Figure 4.

Through this figure, we note that this method is very simple, uncomplicated and can be accomplished easily. This method is preferable in the case of a multi-level inverter. Theprincipal disadvantage of the SVPWM strategy is that the THD value of voltages/currents is high.

To overcome the problems of the traditional four-level SVPWM strategy, the ANN algorithms are designed and used in this study to command the rotor converter of DFIG-DRWT. However, the ANN method has found many applications such as command AC machines.The ANN algorithm contains an output layer, input layer, and hidden layer Madvar et al. (2020). The ANN controller is a method based on observations and engineering experience. In neural techniques, we do not need the mathematical model of the systems compared with another classical strategy. The design of a four-level SVPWM strategy that incorporates the neural method allows minimizing the THD value, increasing robustness and reducing the ripples of DFIG-DRWT powers.

Table 2. Comparative study between the traditional SVM
and the proposed SVM in Benbouhenni (2020b).

	Traditional SVM	Proposed SVM in Benbouhenni (2020b)
Simplicity	Complicated	Simple
Implementation	Complicated	Easy
Applied to multi-level inverter	Difficult	Easily
Robustness	Robust	Robust
Calculate of the sector and angle	Yes	No
Dynamic response	Slow	Fast
Energy	High	Low
Circuit size	Big	Small
Completion cost	Expensive	Not expensive
THD	Medium	Medium
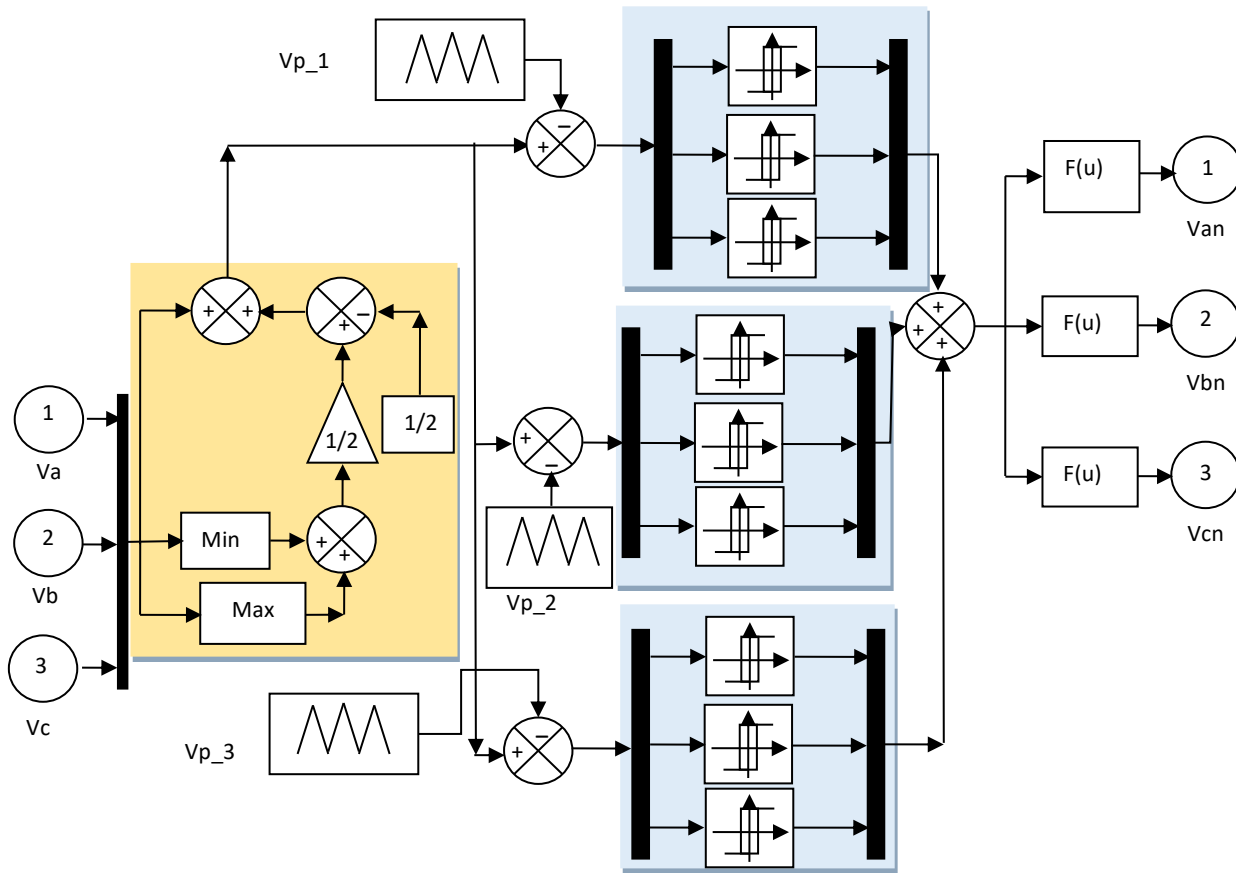
Figure 4. Four-level SVPWM strategy.
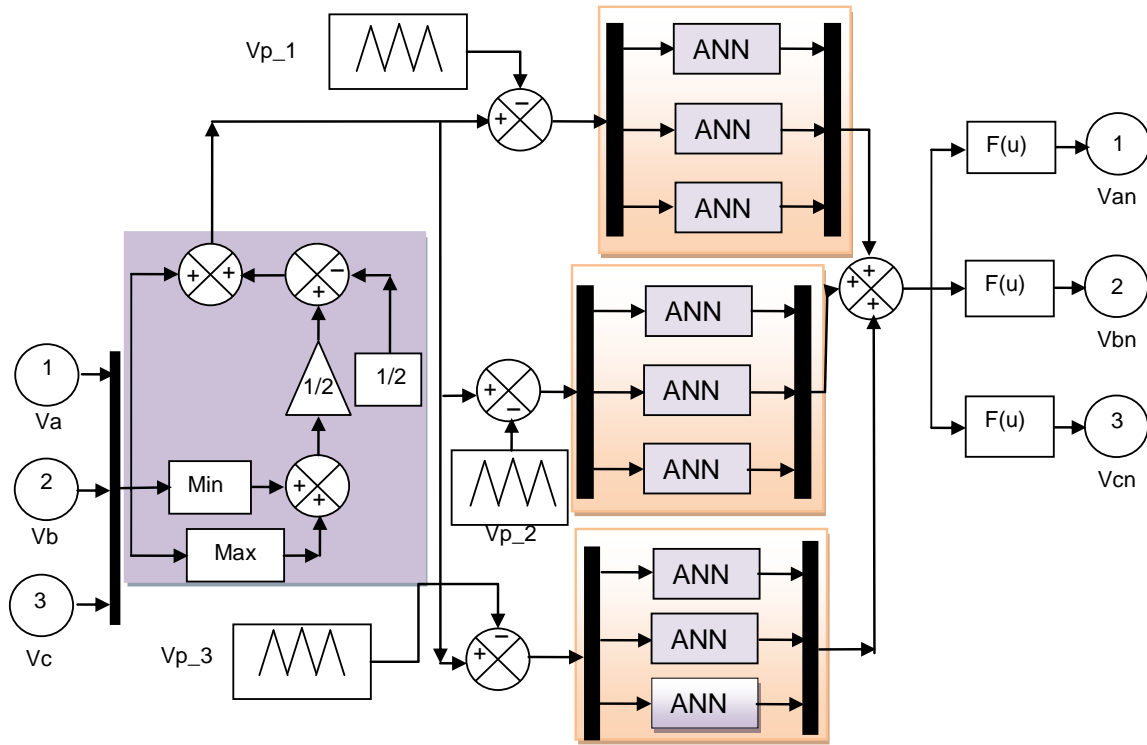
Figure 5. Four-level neural SVPWM strategy.

On the other hand, unlike the classical method, this proposed method is less expensive and therefore can be easily accomplished (criteria that are decisive in choosing a control method).

In the four-level neural SVPWM strategy, the training used is that of the Levenberg-Marquardt (LM) algorithm. The parameters of the LM algorithm are shown in Table 3. The structure of the ANN algorithm is shown in Figure 6. In addition, the structure of layer 1 and layer 2 is shown in Figure 7 and Figure 8, respectively.

Figure 7. Structure of the layer 1.

Figure 8. Structure of the layer 2.
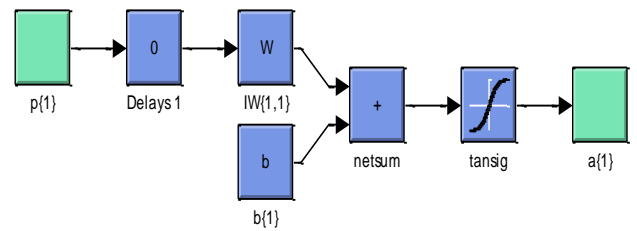

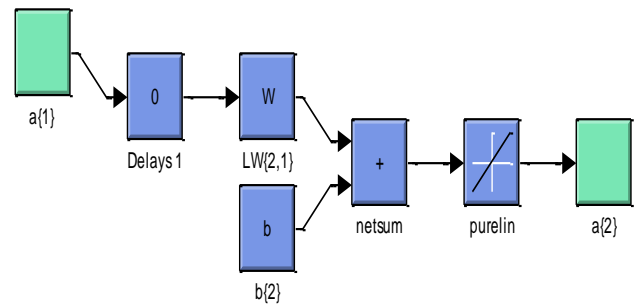Figure 6. Structure interne of the neural hysteresis controllers.

Table 3. Parameters of the LM algorithm

Parameters of the LM algorithm	Values
Functions of activation	Tensing, Purling, Gensim
Number of neurons of input layer	1
Train Param.Lr	0.02
Train Param.eposh	300
Number of neurons of hidden layer	8
Train Param.show	50
Coeff of acceleration of convergence(mc)	0.9
Train Param.mu	0.9
Number of hidden layers	1
Number of neurons of output layer	1
TrainParam.goal	0

The method proposed in this section is used to better control a 4-level NPC inverter of the DFIG-DRWT system. Due to the use of the neural PI controller, a more robust method is obtained, thus reducing current and active power fluctuations.

2.4. Neural DPC strategy with four-level NSVPWM technique

The operating diagram of the neural DPC with four-level NSVPWM strategy (NDPC-4L-NSVPWM) is presented in Figure 9. The novelty and difference compared to DPC-PI strategy is using of the four-level NSVPWM technique to replace the classical SVPWM technique and neural controllers to replace the classical PI controllers. This designed command technique is a robust algorithm and easy to implement. The main advantages of neural DPC with 4L-NSVPWM technique are its good dynamic response, simple algorithm, and constant switching frequency operation. Also, this strategy gives minimum powers undulations and THD of rotor voltage of the DFIG-DRWT compared to the vector control and DPC-PI strategy.

In neural PI controller, the training used is that of the retro-propagation of LM algorithm. The components of the LM method are shown in Table 4. The structure of the ANN controller is shown in Figure 10. On the other hand, the structure of the layer 1, layer 2 and hidden layer is shown in Figure 11, Figure 12 and Figure 13 respectively.
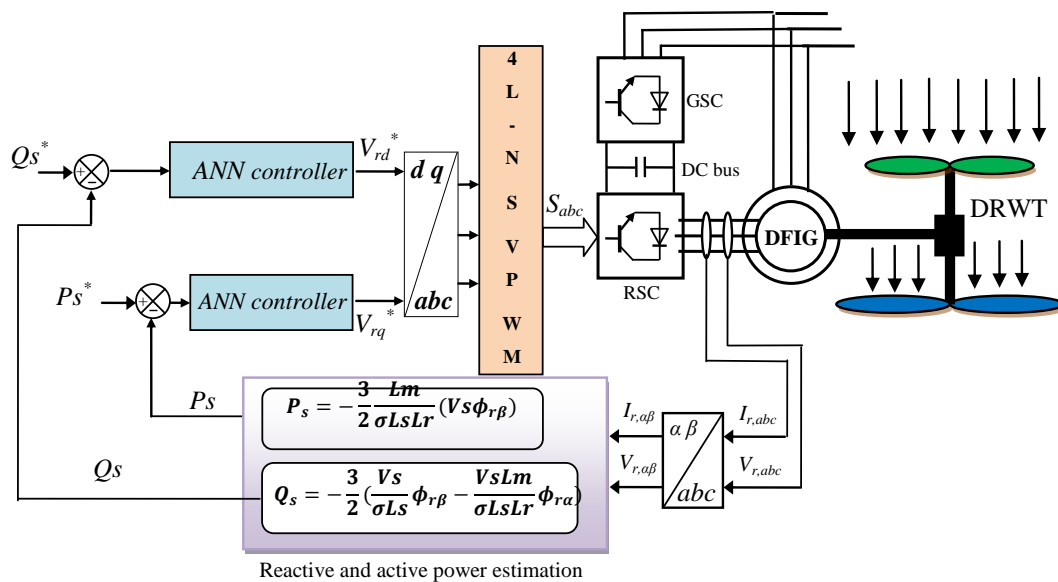

Reactive and active power estimation

$$P_s = -\frac{3}{2}\frac{Lm}{\sigma LsLr}(Vs\phi_{r\beta})$$

$$Q_s = -\frac{3}{2}(\frac{Vs}{\sigma Ls}\phi_{r\beta} - \frac{VsLm}{\sigma LsLr}\phi_{r\alpha})$$

Figure 9. NDPC strategy with four-level neural SVPWM strategy.

Table 4. Characteristics of the retro-propagation.

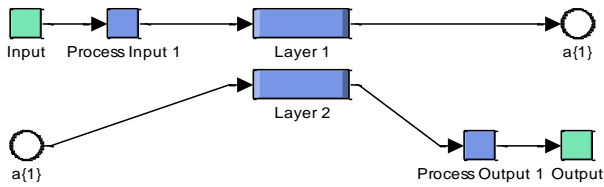| Parameters of the LM	Values
Train Param.eposh	1000
TrainParam.Lr	0.005
Train Param.show	50
Number of input layer	1
Train Param.goal	0
Number of output layer	1
Train Param.mu	0.9
Coeff of acceleration of convergence (mc)	0.9
Number of hidden layers	1
Functions of activation	Tensing, Purling, Gensim
Number of neurons of hidden layer	8

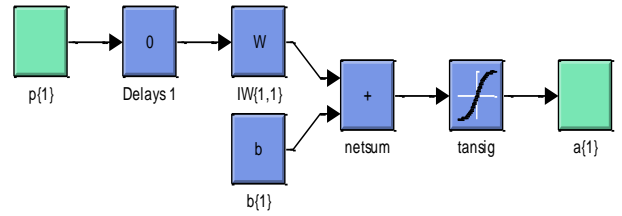
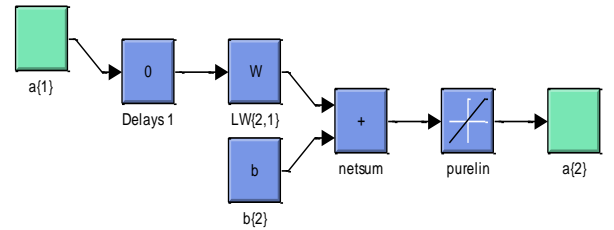Figure 11. Layer 1.

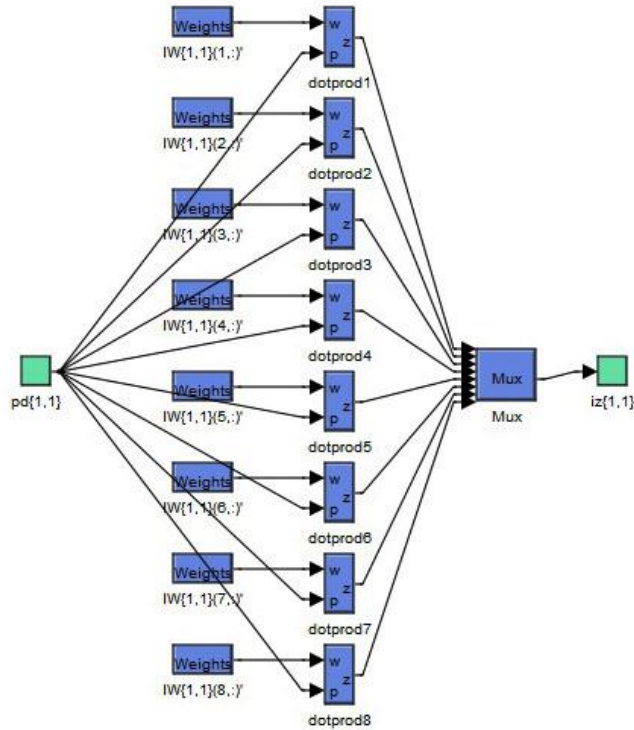Figure 12. Layer 2.

Figure 10. ANN controller.

Figure 13. Hidden layer.

3. Results

Numerical simulations for the validation of strategies designed for a DFIG-DRWT have been performed in Matlab.The parameters of machine are those mentioned in Benbouhenni and Bizon (2021b), (2021c) and presented in Annex A1. The parameters of the PI regulators of the reactive and active powers as shown in Table 5. Both methods will be tested and compared in two different tests: reference tracking and robustness tests.

Table 5. PI controller gains.

Active power		Reactive power	
Ki	Kp	Ki	Kp
1000	100	1000	100

A. The first test

The first test(T1) is the reference tracking test. The goal is to find out which method provides better results in terms of reference tracking. Also, in terms of ripple value and THD value. By using simulation, the results are shown in the Figures 14 to 23. Figures 18-19 show the THD value of current for both strategies of DFIG-DRWT. Note that the THD value is reduced for NDPC-4L-NSVPWM when compared to DPC-PI technique (Table 6). Through this table, we find that the proposed NDPC-4L-NSVPWM strategy minimized the THD value of stator current by about 76.66% compared to the DPC-PI technique.

Table 6. THD value of both techniques.

	THD (%)	
	DPC-PI	NDPC-4L-NSVPWM
Current (*Ias*)	1.50	0.35

The simulation signal of the measured and reference reactive power of the DFIG-DRWT are shown in Figure 15 in order to compare the characteristics of the NDPC strategy with application of the 4L-NSVPWM technique with the characteristics of the conventional DPC-PI strategy. The reactive power track well their reference value (*Qs-ref*). The designed technique give minimum the oscillations of the reactive power relative to the classical DPC with PI controllers (Figure 21).

For both strategies, the active power track well their reference value (see Figure 14). Moreover, the DPC-4L-NSVPWM strategy reduced the active power ripple relative to the DPC-PI (Figure 20).

The simulation waveforms of the measured torque of the three-phase DFIG are presented in Figure 16 to compare the characteristics and effectiveness of the NDPC technique using the 4L-NSVPWM technique with those obtained using the DPC-PI strategy. The NDPC-4L-NSVPWM method reduces the torque ripple in comparison with the DPC-PI technique (Figure 22).

The shape of the current (Ias) is presented in Figure 17. It is observed that the amplitudes of Ias depend on the value of the DFIG-DRWT load. Note that the NDPC-4L-NSVPWM method minimized the current oscillations relative to the DPC-PI technique (Figure 23).

Table 7 shows the values of the response time for the active power and electromagnetic torque of both DPC strategies. From this table, we not that the NDPC strategy with 4L-NSVPWM technique is the best in terms reduce of the response time (less time). Through these results, it is noted that the proposed NDPC-4L-NSVPWM technique minimized the value of the time response for each of the torque and active power about 29% and 31.5%, respectively, compared to the DPC-PI technique.

Table 7. Comparative analysis of response time.

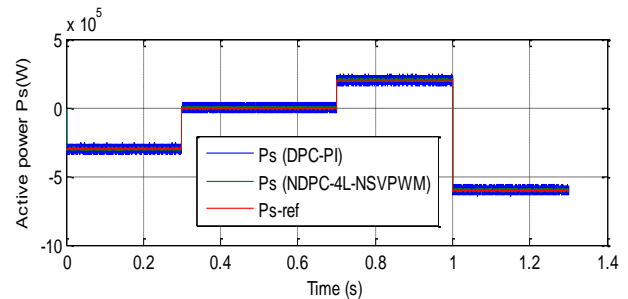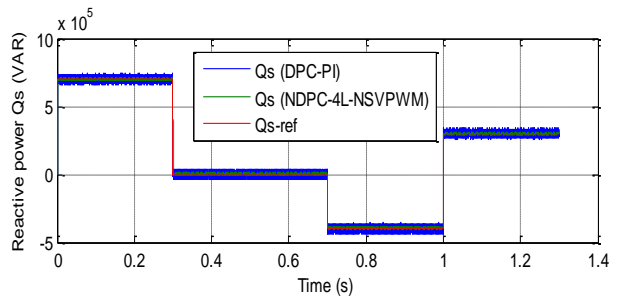|	Response time (ms)	
	DPC-PI	NDPC-4L-NSVPWM
Active power	0.200	0.137
Torque	0.200	0.142

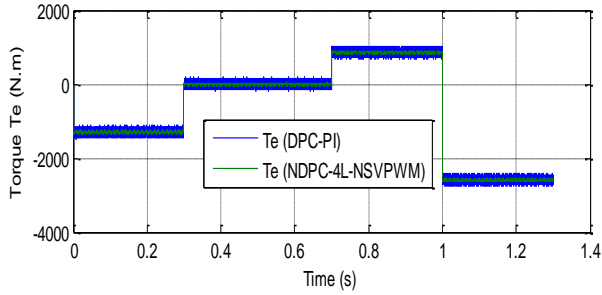
Figure 14. Active power.

Figure 15. Reactive power.

Figure 16. Torque.

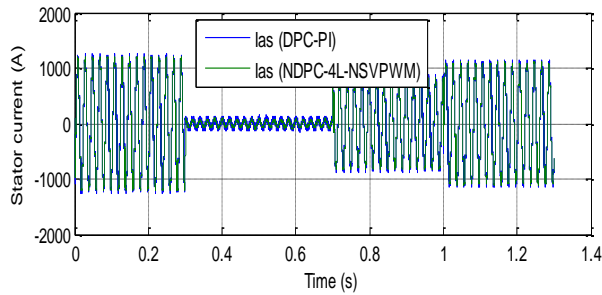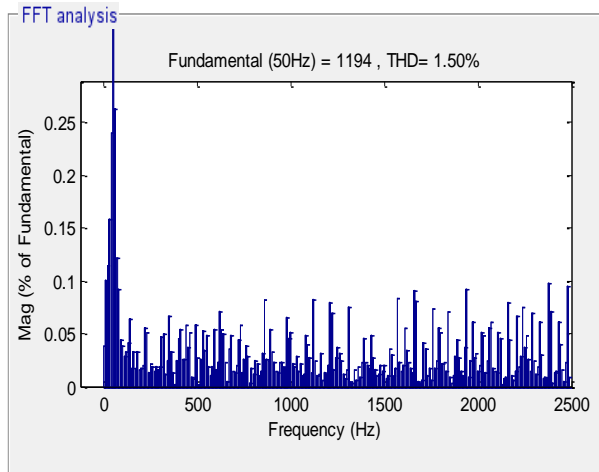
Figure 17. Stator current.
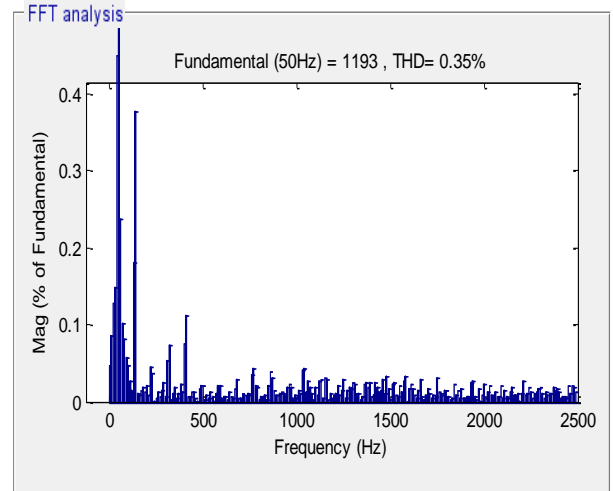

Figure 18. THD value of the *Ias* (DPC-PI).

Figure 19. THD value of the *Ias* (NDPC-4L-NSVPWM).

The zoom in the active power, reactive power, torque and stator current is shown in Figures 20 to 23, respectively. It can be seen that the NDPC strategy with 4L-NSVPWM technique reduced the oscillations in active power, reactive power, torque and stator current relative to the DPC with PI controllers.
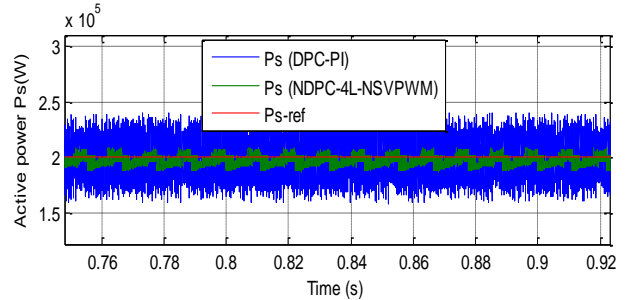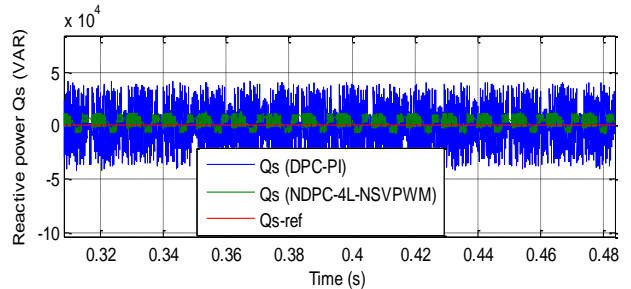

Figure 20. Zoom (*Ps*).

Figure 21. Zoom (*Qs*).
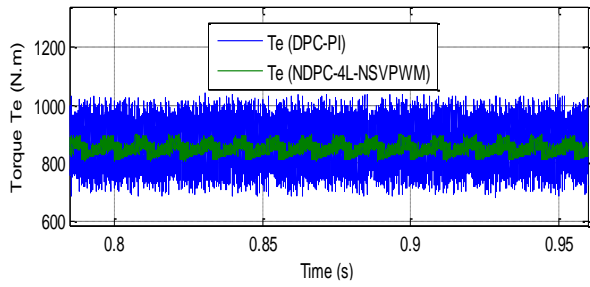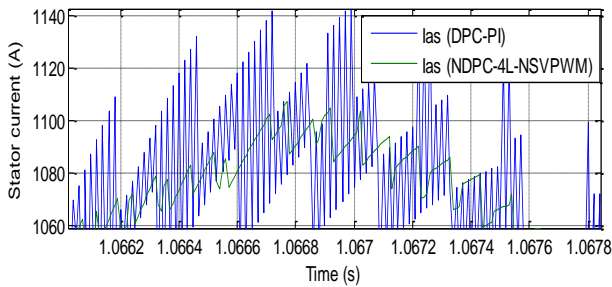
Figure 22. Zoom (*Te*).

Figure 23. Zoom (*Ias*).

The results of the first test are summarized in Table 8. Table 8 represents a comparative study between the DPC-PI strategy and the proposed strategy in terms of response time, reference tracking, effective power ripple value, THD value, etc. Through this table, it is concluded that the designed strategy is much better than the DPC-PI strategy. The designed strategy improved the efficiency and features of the machine such as setting time and time response.

Table 8. Comparative results obtained from the designed.

Criteria	Control strategies	
	DPC-PI	NDPC-4L-NSVPWM
Reference power tracking	Acceptable	Very good
THD (%)	1.50	0.35
Power ripples	High	Low
Time response (s)	Medium	Low
Qs: ripples (VAR)	About 80000	About 1200
Te: ripple (N.m)	About 300	About 20
Settling time (ms)	Medium	Low

Overshoot (%)	≈ 24%	≈ 1.3%
Robustness	Medium	High
Ps: ripples (W)	About 75000	About 1350
Converter and filter design	Simple	Simple
Rise time (s)	Medium	Low
Ias: ripple (A)	About 80	About 20
Algorithm complexity	Simple	Simple
Dynamic performance	Slow	Fast
Quality of the current/power generated	Acceptable	Excellent

B. The second test

The second test (T2) is the robustness test. In this test, the values used in the first test for the Rr and Rs are multiplied by 2, and the values for the Lr and Ls are multiplied by 0.5, where Rr and R_s are the resistances, and Lr and Ls are the inductance of the stator and rotor windings mentioned in Annex A1. Simulation results are presented in Figures 24-33. As it's shown by these figures, the reactive and active power tracks well their reference values (see Figure 26-27). Figures 28 and 29 show the torque and current, respectively. From this figures, torque and current deponds the system and load active power. In addition, these variations present an apparent effect on reactive power, torque, active power and currents curves such as the effect appears more significant for the DPC-PI strategy relative to NDPC-4L-NSVPWM (see Figures 30-33).

The THD of current in the NDPC-4L-NSVPWM technique has been reduced significantly (Figures 24-25). Table 9 shows the THD values of both strategies. Through this table, we find that the proposed NDPC-4L-NSVPWM technique reduced the THD value by about 79.27% compared to the DPC-PI technique. Based on the results presented here, it can be concluded that the designed NDPC-4L-NSVPWM strategy is more robust than the traditional DPC-PI method.

Table 9. THD value of both techniques.

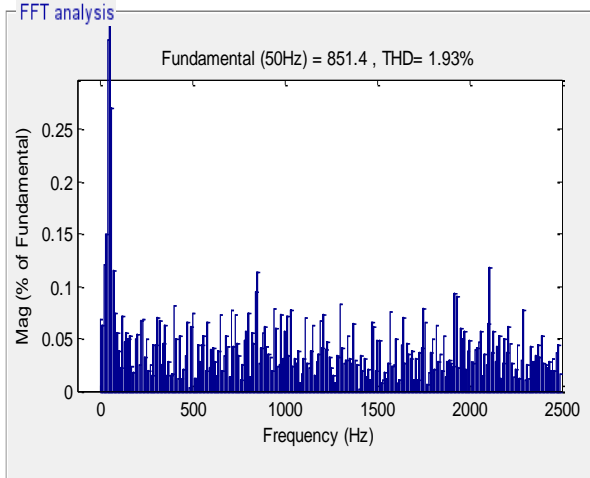|	THD (%)	
	DPC-PI	NDPC-4L-NSVPWM
Current (*Ias*)	1.93	0.40

Figure 24. THD value of the *Ias* (DPC-PI).
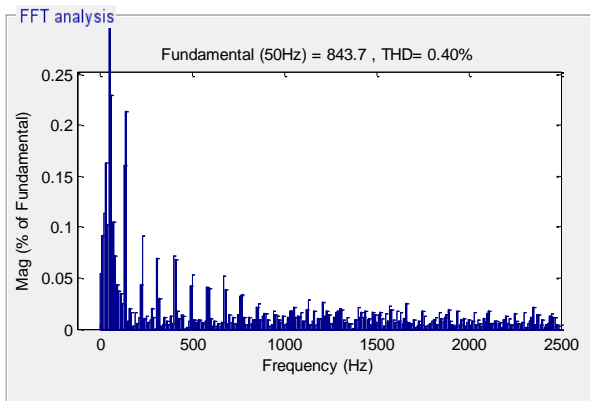
Figure 25. THD value of the *Ias* (NDPC-4L-NSVPWM).

Figure 26. Active power.

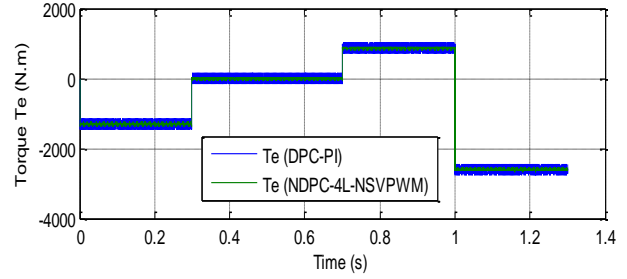Figure 27. Reactive power.

Figure 28. Torque.
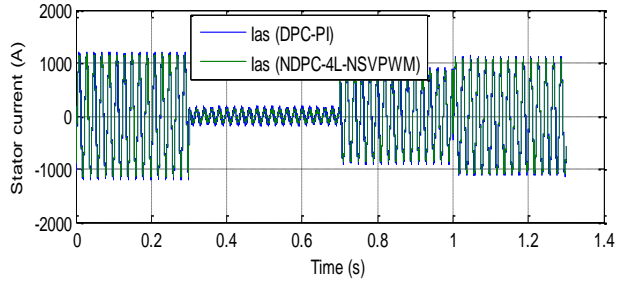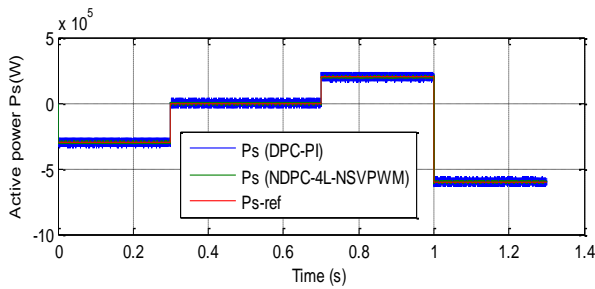

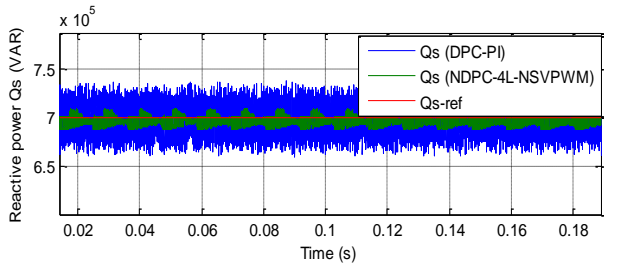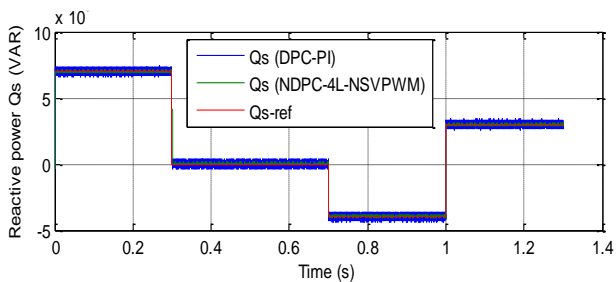Figure 29. Stator current.
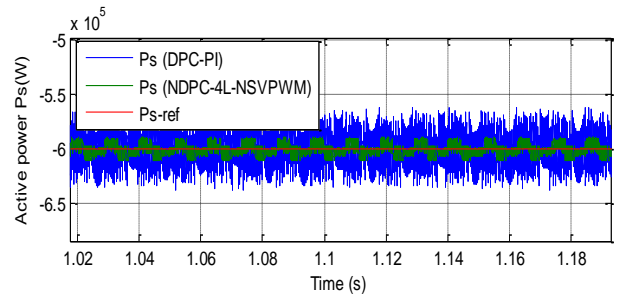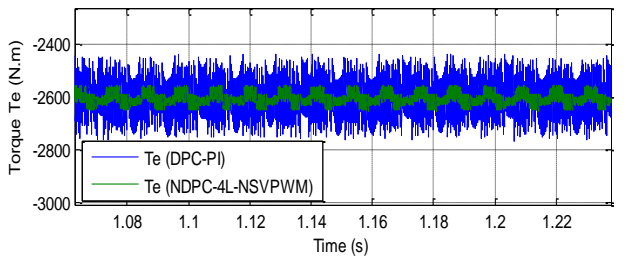

Figure 30. Zoom (*Ps*).
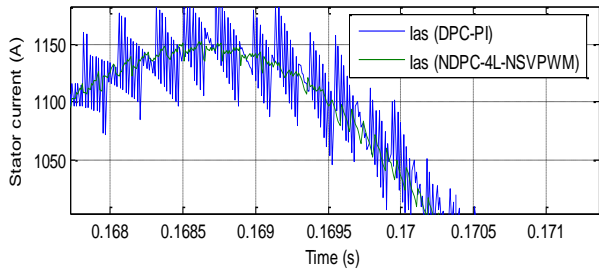

Figure 31. Zoom (*Qs*).

Figure 32. Zoom (*Te*).

Figure 33. Zoom (*Ias*).

A comparative study between the designed NDPC-4L-NSVPWM in this work with some published works in terms of the value of THD is shown in Table 10. Through this table, we notice that this NDPC-4L-NSVPWM technique gave for the THD of the current a better value compared to other control methods.

Table 10. Comparison of the obtained results with those reported in reference control schemes proposed in the literature.

References	Strategies	THD (%)
Boudjema et al. (2017)	Direct torque control	2.57
	DTC-SOCSM strategy	0.98
Jbarah and Andrey (2021)	DTC-PI strategy	0.63
Ayrir et al. (2020)	DTC strategy	6.70
	Fuzzy DTC strategy	2.04
Boudjema et al. (2013)	Fuzzy sliding mode controller technique	3.1
Yaichi et al. (2019)	DPC with STA algorithm	1.66
Amran and Chaiba (2016)	FOC strategy	3.70
Alhato and Bouallègue (2019)	DPC control using L-filter	10.79
	DPC control using LCL-filter	4.05
Quan et al. (2019)	Integral SMC technique	9.7
	Multi-resonant-based SMC	3.2
Boudjema et al. (2016)	SOSMC method	3.13
Jbarah and Mazalov (2021)	DTC-PI strategy	0.88
	DTC-STA technique	0.59
Yusoff et al. (2017)	Virtual flux DPC strategy	4.2
	DPC	4.9
Proposed strategies	DPC-PI	1.50
	NDPC-4L-NSVPWM	0.35

Response time for the designed technique and that obtained in the paper published in Yaichi et al. (2020) are recorded in Table 11. Through this table, we find that the proposed NDPC-4L-NSVPWM strategy gave a very fast time response compared to the two proposed methods in Yaichi et al. (2020), where we find that the proposed NDPC-4L-NSVPWM

strategy improved the time response for the torque by about 97.16% and 99.21% compared to the neuro-second order SMC technique and DPC strategy, respectively, and for active power by about 97.26% and 99.23% compared to the neuro-second order SMC technique and DPC strategy, respectively. It can be concluded from Tables 10 and 11 that the proposed NDPC-4L-NSVPWM strategy can be used to ameliorate the quality of the power and the current produced by the DFIG-DRWT systems.

Table 11. Comparative analysis of response time.

		Response time	
		Torque	Active power
	Designed strategy: NDPC-4L-NSVPWM	0.142 ms	0.137 ms
Yaichi et al. (2020)	Neuro-second order SMC technique	5 ms	5 ms
	Direct power control	18 ms	18 ms

A comparative study has been performed between the designed technique in this work with both field-oriented control with PI controllers (FOC-PI) and integral SMC (ISMC) technique proposed in (Chojaa et al., 2021) in terms of response time, THD value, and reactive power ripples value. Table 12 represents this comparative study between the designed technique and the FOC-PI and ISMC strategies. By analyzing this table, we find that the projected technique is better than the FOC-PI and ISMC strategies in most criteria, except for the THD value for current, where a value comparable to that given by the ISMC strategy is obtained.

Table 12. Comparative analysis of both strategies (FOC-PI, ISMC and proposed strategy)

		THD (%)	Response time (s)	Overshoot (%)	Reactive power: ripples (VAR)	Precision
	Designed strategy: NDPC-4L-NSVPWM	0.35	0.137	≈ 1.3%	1200	High
Chojaa et al. (2021)	FOC-PI	1.33	0.408	≈ 16%	12500	Medium
	ISMC	0.27	0.280	≈ 5%	3100	High

4. Discussion

The ripples' reduction is estimated by the reduction ratio of the THD value (THDR), the current ripple reduction ratio.

(CRRR), the torque ripple reduction ratio (TRRR), and active power ripple reduction ratio (PRRR) given by Equations (16) and (19):

$$THDRi\ (\%) = \frac{THD_{S_1Ti} - THD_{S_2Ti}}{THD_{S_1Ti}} \tag{16}$$

$$CRRRi\ (\%) = \frac{I_{erS_1Ti} - I_{erS_2Ti}}{I_{erS_1Ti}} \tag{17}$$

$$TRRRi\ (\%) = \frac{T_{erS_1Ti} - T_{erS_2Ti}}{T_{erS_1Ti}} \tag{18}$$

$$PRRRi\ (\%) = \frac{P_{erS_1Ti} - P_{erS_2Ti}}{P_{erS_1Ti}} \tag{19}$$

where I_{erS_1Ti}, T_{erS_1Ti} and P_{erS_1Ti} represent the ripples' value for the current, torque and active power of the classical strategy (S1), and I_{erS_2Ti}, T_{erS_2Ti} and P_{erS_2Ti} represents the ripples' value for the same variables of the proposed strategy (S2), under the both tests (Ti,i=1,2) mentioned above.

The reduction ratios will be estimated for the first and second tests (without and with changes in the parameters of the generator) to evaluate the robustness of the analyzed strategies.

Considering the results presented in the first test (T1), the reduction rate for the ripples in stator current (CRRR1), torque (TRRR1), and active power (PRRR1) is approximated at about 82%, 80%, and 75%, respectively, using (16)-(19). Also, the THD value for the designed NDPC-4L-NSVPWM strategy and classic DPC-PI technique is of 0.35% and 1.5%. Thus, the THD reduction (THDR1) can be approximated at about 76.67% using (16).

On the same manner, using (16)-(19) and the results presented in the second test (T2), the values of the CRRR2, TRRR2 and PRRR2 can be approximated at about 80%, 81.43%, and 75%, respectively. Also, the THD value for the designed NDPC-4L-NSVPWM strategy and classic DPC-PI technique is of 0.4% and 1.93%. Thus, THDR2 can be approximated at about 79.28% using (16).

The THD and the torque ripple are estimated in both tests using the strategies Sj, j=1,2, where S1 and S2 means the DPC-PI strategy and NDPC-4L-NSVPWM strategy, respectively. The obtained values are used below to assess robustness based on the two indicators defined in Table 13.

Table 13. Comparison of the effect ratio of proposed and classical control methods.

Robustness indicator	Designed control techniques	
	DPC-PI	NDPC-4L-NSVPWM
$\frac{THD_{Sj(T1)} - THD_{Sj(T2)}}{THD_{Sj(T1)}}$ [%]	28.67	14.29
$\frac{T_{er1Sj(T1)} - T_{er1Sj(T2)}}{T_{er1Sj(T1)}}$ [%]	16.67	8.33

The values mentioned in table above clearly highlight that the proposed NDPC-4L-NSVPWM technique is less affected compared to the DPC-PI technique.

5. Conclusion

In this work, the NDPC-4L-NSVPWM strategy is proposed, designed and analyzed as performance compared to the DPC-PI technique. The results obtained for the ripple's values of current, power and torque and THD values of the variables mentioned above, highlight the performance of the NDPC-4L-NSVPWM technique compared to the DPC-PI technique, the reference works considered in summary tables and other recent works such as Benbouhenni and Bizon (2021b), (2021c), Madvar et al. (2020), Yaichi et al. (2020), Benbouhenni (2021a), (2021b). The main findings are as follows:

-A new NDPC-4L-NSVPWM technique was proposed and designed.

-The proposed NDPC-4L-NSVPWM technique is much more robust compared to the DPC-PI technique; the values of the robustness indicators mentioned in Table 13 is about half for NDPC-4L-NSVPWM technique compared to the DPC-PI technique.

-Minimization of ripples for electromagnetic torque, rotor current and active power has been shown; in both tests, the reduction rate of the ripples in the stator current and the torque is about 80%, and the reduction rate of the active power is about 75%; Thus, the THD reduction is approximately 76.67% and 79.28% in the first and second test.

The following work will be devoted to experimental implementation and validation of the NDPC-4L-NSVPWM strategy.

Appendix A

The values of the parameters used in the first test are mentioned in Table A1.

Table A1. The values of the parameters used in simulation

Vn	380 V
Pn	1.5 MW
p	2
J	1000 Kg.m2
Rs	0.012 Ω
Rr	0.021 Ω
Ls	0.0137 H
Lr	0.0136 H
Lm	0.0135 H

Conflict of interest

The authors have no conflict of interest to declare.

Funding

The authors received no specific funding for this work.

References

Alhato, M. M., & Bouallègue, S. (2019). Direct power control optimization for doubly fed induction generator based wind turbine systems. *Mathematical and Computational Applications*, *24*(3), 77.
https://doi.org/10.3390/mca24030077

Amrane, F., & Chaiba, A. (2016). A novel direct power control for grid-connected doubly fed induction generator based on hybrid arti ficial intelligent control with space vector modulation. Rev. Roum. Sci. Techn. 61(3), 263-268.

Amrane, F., Chaiba, A., Babes, B. E., & Mekhilef, S. (2016). Design and implementation of high performance field oriented control for grid-connected doubly fed induction generator via hysteresis rotor current controller. Rev. Roum. Sci. Techn.-Electrotechn. Et Energ, 61(4), 319-324.

Ayrir, W., Ourahou, M., El Hassouni, B., & Haddi, A. (2020). Direct torque control improvement of a variable speed DFIG based on a fuzzy inference system. *Mathematics and Computers in Simulation*, *167*, 308-324.
https://doi.org/10.1016/j.matcom.2018.05.014

Benbouhenni, H., Boudjema, Z., & Belaidi, A. (2018). Sensorless twelve sectors implementation of neural DPC controlled DFIG for reactive and active powers ripples reduction. Majlesi Journal of Energy Management, 7(2), 13-21.

Benbouhenni, H. (2019). Application of five-level NPC inverter in DPC-ANN of doubly fed induction generator for wind power generation systems. *International Journal of Smart Grid*, *3*(3), 128-137.
https://doi.org/10.20508/ijsmartgrid.v3i3.66.g59

Benbouhenni, H. (2020a). Twelve sectors DPC control based on neural hysteresis comparators of the DFIG integrated to wind power. *Tecnica Italiana-Italian Journal of Engineering Science*, *64*(2), pp. 347-353.
https://doi.org/10.18280/ti-ijes.642-433

Benbouhenni, H. (2020b). ANFIS-sliding mode control of a DFIG supplied by a two-level SVPWM technique for wind energy conversion system. *International Journal of Applied Power Engineering*, *9*(1), 36-47.
https://doi.org/10.11591/ijape.v9.i1.pp36-47

Benbouhenni, H., Boudjema, Z., & Belaidi, A. (2020). DPC based on ANFIS super-twisting sliding mode algorithm of a doubly-fed induction generator for wind energy system. *Journal Européen des Systèmes Automatisés*, *53*(1), 69-80.
https://doi.org/10.18280/jesa.530109

Benbouhenni, H., Boudjema, Z., & Belaidi, A. (2021). Direct power control with NSTSM algorithm for DFIG using SVPWM technique. *Iranian Journal of Electrical & Electronic Engineering*, *17*(1), 1-11.
https://doi.org/10.22068/IJEEE.17.1.1518

Benbouhenni, H. (2021a). Intelligent super twisting high order sliding mode controller of dual-rotor wind power systems with direct attack based on doubly-fed induction generators. Journal of Electrical Engineering, Electronics, Control and Computer Science, 7(4), 1-8.

Benbouhenni, H. (2021b). Synergetic control theory scheme for asynchronous generator based dual-rotor wind power. Journal of Electrical Engineering, Electronics, Control and Computer Science, 7(3), 19-28.

Benbouhenni, H., & Bizon, N. (2021a). Third-order sliding mode applied to the direct field-oriented control of the asynchronous generator for variable-speed contra-rotating wind turbine generation systems. *Energies*, *14*(18), 4437.
https://doi.org/10.3390/en14185877

Benbouhenni, H., & Bizon, N. (2021b). Improved rotor flux and torque control based on the third-order sliding mode scheme applied to the asynchronous generator for the single-rotor wind turbine. *Mathematics*, 9(18), 2297. https://doi.org/10.3390/math9182297

Benbouhenni, H., & Bizon, N. (2021c). A synergetic sliding mode controller applied to direct field-oriented control of induction generator-based variable speed dual-rotor wind turbines. *Energies*, 14(15), 4437. https://doi.org/10.3390/en14154437

Bouyekni, A., Taleb, R., Boudjema, Z., & Kahal, H. (2018). A second-order continuous sliding mode based on DPC for wind-turbine-driven DFIG. Elektrotehniski Vestnik, 85(1/2), 29-36.

Boudjema, Z., Meroufel, A., Djerriri, Y., & Bounadja, E. (2013). Fuzzy sliding mode control of a doubly fed induction generator for wind energy conversion. Carpathian Journal of Electronic and Computer Engineering, 6(2), 7-14.

Boudjema, Z., Hemici, B., & Yahdou, A. (2016). Second order sliding mode control of a dual-rotor wind turbine system by employing a matrix converter. Journal of Electrical Engineering, 16(3), 11-11.

Boudjema, Z., Taleb, R., Djeriri, Y., & Yahdou, A. (2017). A novel direct torque control using second order continuous sliding mode of a doubly fed induction generator for a wind energy conversion system. *Turkish Journal of Electrical Engineering and Computer Sciences*, 25(2), 965-975. https://doi.org/10.3906/elk-1510-89

Chen, S. Z., Cheung, N. C., Wong, K. C., & Wu, J. (2009). Integral sliding-mode direct torque control of doubly-fed induction generators under unbalanced grid voltage. *IEEE transactions on energy conversion*, 25(2), 356-368. https://doi.org/10.1109/TEC.2009.2036249

Chojaa, H., Derouich, A., Chehaidia, S. E., Zamzoum, O., Taoussi, M., & Elouatouat, H. (2021). Integral sliding mode control for DFIG based WECS with MPPT based on artificial neural network under a real wind profile. *Energy Reports*, 7, 4809-4824. https://doi.org/10.1016/j.egyr.2021.07.066

Djeriri, Y. (2020). Lyapunov-based robust power controllers for a doubly fed induction generator. *Iranian Journal of Electrical and Electronic Engineering*, 16(4), 551-558. https://doi.org/10.22068/IJEEE.16.4.551

Djilali, L., Sanchez, E. N., & Belkheiri, M. (2020). First and high order sliding mode control of a dfig-based wind turbine. *Electric Power Components and Systems*, 48(1-2), 105-116. https://doi.org/10.1080/15325008.2020.1758836

El Ouanjli, N., Derouich, A., El Ghzizal, A., Taoussi, M., El Mourabit, Y., Mezioui, K., & Bossoufi, B. (2019). Direct torque control of doubly fed induction motor using three-level NPC inverter. *Protection and Control of Modern Power Systems*, 4(1), 1-9. https://doi.org/10.1186/s41601-019-0131-7

Farajpour, Y., Alzayed, M., Chaoui, H., & Kelouwani, S. (2020). A Novel Switching Table for a Modified Three-Level Inverter-Fed DTC Drive with Torque and Flux Ripple Minimization. *Energies*, 13(18), 4646. https://doi.org/10.3390/en13184646

Izanlo, A., Gholamian, S. A., & Kazemi, M. V. (2017). Comparative study between two sensorless methods for direct power control of doubly fed induction generator. Â» Rev. Roum. Sci. Techn.-Electrotechn. Et Energ, 62(4), 358-364.

Jazaeri, M., Samadi, A. A., Najafi, H. R., & Noroozi-Varcheshme, N. (2012). Eigenvalue Analysis of a Network Connected to a Wind Turbine Implemented with a Doubly-Fed Induction Generator (DFIG). *Journal of applied research and technology*, 10(5), 791-811. https://doi.org/10.22201/icat.16656423.2012.10.5.375

Jbarah, A. A. N., & Andrey, M. (2021). Improved dfig dftc by using a fractional-order super twisting algorithms in wind power application. *Transportation Systems and Technology*, 7(3), 131-149. https://doi.org/10.17816/transsyst202173131-149

Jbarah, A. A. N. & Mazalov, A. A. (2021). Improving the efficiency of direct flux and torque control technology for doubly-fed induction generator with a robust control using modified super-twisting algorithms *Vestnik Gosudarstvennogo universiteta morskogo i rechnogo flota imeni admirala S. O. Makarova*, 13(4), 586-603. https://doi.org/10.21821/2309-5180-2021-13-4-586-603

Jou, S. T., Lee, S. B., Park, Y. B., & Lee, K. B. (2009). Direct power control of a DFIG in wind turbines to improve dynamic responses. Journal of power electronics, 9(5), 781-790.

Kulothungan, G. S., Edpuganti, A., Rathore, A. K., Rodriguez, J., & Srinivasan, D. (2019). Hybrid SVM-SOPWM modulation of current-fed three-level inverter for high power application. *IEEE Transactions on Industry Applications*, 55(4), 4344-4358. https://doi.org/10.1109/TIA.2019.2912967

Luo, X., & Niu, S. (2017). A novel contra-rotating power split transmission system for wind power generation and its dual MPPT control strategy. *IEEE Transactions on Power Electronics*, *32*(9), 6924-6935. https://doi.org/10.1109/TPEL.2016.2629021

Madvar, H. R., Dehghani, M., Memarzadeh, R., Salwana, E., Mosavi, A., & Shahab, S. (2020). Derivation of optimized equations for estimation of dispersion coefficient in natural streams using hybridized ANN with PSO and CSO algorithms. *IEEE Access*, *8*, 156582-156599. https://doi.org/10.1109/ACCESS.2020.3019362

Muller, S., Deicke, M., & De Doncker, R. W. (2002). Doubly fed induction generator systems for wind turbines. *IEEE Industry applications magazine*, *8*(3), 26-33. https://doi.org/10.1109/2943.999610

Mirzakhani, A., Ghandehari, R., & Davari, S. A. (2018). A new DPC-based control algorithm for improving the power quality of DFIG in unbalance grid voltage conditions. International Journal of Renewable Energy Research, 8(4), 2228-2238.

Mondal, S., & Kastha, D. (2019). Input reactive power controller with a novel active damping strategy for a matrix converter fed direct torque controlled DFIG for wind power generation. *IEEE Journal of Emerging and Selected Topics in Power Electronics*, *8*(4), 3700-3711. https://doi.org/10.1109/JESTPE.2019.2938012

Mossa, A. M., Echeikh, H., Diab, A. A. Z., & Quynh, N. V. (2020). Effective direct power control for a sensor-less doubly fed induction generator with a losses minimization criterion. *Electronics*, *9*(8), 1269. https://doi.org/10.3390/electronics9081269

Mekkaoui, N., & Naït-Saïd, M. (2017). Direct s-power control for a doubly fed induction generator. Rev. Roum. Sci. Techn.- Electrotechn. Et Energ, 62(4), 365-370.

Phan, D. C., & Yamamoto, S. (2015). Maximum energy output of a DFIG wind turbine using an improved MPPT-curve method. *Energies*, *8*(10), 11718-11736. https://doi.org/10.3390/en81011718

Quan, Y., Hang, L., He, Y., & Zhang, Y. (2019). Multi-resonant-based sliding mode control of DFIG-based wind system under unbalanced and harmonic network conditions. *Applied Sciences*, *9*(6), 1124. https://doi.org/10.3390/app9061124

Rodarte Gutiérrez, F. E., Carranza Castillo, O., Rodríguez Rivas, J. J., Ortega González, R., Peralta Sánchez, E., & González Morales, L. G. (2021). Harmonics reduction and reactive power injection in wind generation systems. *Electronics*, *10*(16), 1964. https://doi.org/10.3390/electronics10161964

Shehata, E. G., & Salama, G. M. (2013). Direct power control of DFIGs based wind energy generation systems under distorted grid voltage conditions. *International Journal of Electrical Power & Energy Systems*, *53*, 956-966. https://doi.org/10.1016/j.ijepes.2013.06.006

Wang, Y., Niu, S., & Fu, W. (2018). A novel dual-rotor bidirectional flux-modulation PM generator for stand-alone DC power supply. *IEEE Transactions on Industrial Electronics*, *66*(1), 818-828. https://doi.org/10.1109/TIE.2018.2849970

Xu, L., & Cartwright, P. (2006). Direct active and reactive power control of DFIG for wind energy generation. *IEEE Transactions on energy conversion*, *21*(3), 750-758. https://doi.org/10.1109/TEC.2006.875472

Xu, L., & Cheng, W. (1995). Torque and reactive power control of a doubly fed induction machine by position sensorless scheme. *IEEE transactions on Industry Applications*, *31*(3), 636-642. https://doi.org/10.1109/28.382126

Yahdou, A., Djilali, A. B., Boudjema, Z., & Mehedi, F. (2020). Improved vector control of a counter-rotating wind turbine system using adaptive backstepping sliding mode. *Journal Européen des Systèmes Automatisés*, *53*(5), 645-651. https://doi.org/10.18280/jesa.530507

Yaichi, I., Semmah, A., & Wira, P. (2020). Neuro-second order sliding mode control of a DFIG based wind turbine system. Journal of Electrical and Electronics Engineering, 13(1), 63-68.

Yaichi, I., Semmah, A., Wira, P., & Djeriri, Y. (2019). Super-twisting sliding mode control of a doubly-fed induction generator based on the SVM strategy. *Periodica Polytechnica Electrical Engineering and Computer Science*, *63*(3), 178-190. https://doi.org/10.3311/PPee.13726

Yousefi-Talouki, A., Zalzar, S., & Pouresmaeil, E. (2019). Direct power control of matrix converter-fed dfig with fixed switching frequency. *Sustainability*, *11*(9), 2604. https://doi.org/10.3390/su11092604

Yusoff, N. A. M., Razali, A. M., Karim, K. A., Sutikno, T., & Jidin, A. (2017). A concept of virtual-flux direct power control of three-phase AC-DC converter. International Journal of Power Electronics and Drive Systems, 8(4), 1776.

Zhao, W., Lipo, T. A., & Kwon, B. I. (2015). A novel dual-rotor, axial field, fault-tolerant flux-switching permanent magnet machine with high-torque performance. *IEEE Transactions on Magnetics*, *51*(11), 1-4. https://doi.org/10.1109/TMAG.2015.2445926

Zhi, D., & Xu, L. (2007). Direct power control of DFIG with constant switching frequency and improved transient performance. *IEEE transactions on energy conversion*, *22*(1), 110-118. https://doi.org/10.1109/TEC.2006.889549